MUSCL-type interpolation shows that the expansion shocks indeed disappear and all of the schemes tested in this Note generate solutions that are smooth and virtually identical to the analytical solution. This implies that it may be generally safe to avoid an expansion shock as long as higher than first-order MUSCL-type upwind differencing is used.

IV. Conclusion

A numerical test case for the Euler equations is presented to examine the performance of several upwind schemes for satisfying the entropy condition. The first-order upwind schemes of Roe,[1] Van Leer,[2] Steger–Warming,[15] and Van Leer–Hänel et al.[3] and Liou's AUSM[4] and AUSM$^+$,[11] Edwards's LDFSS,[12,13] and a modified Zha–Bilgen[6] scheme are tested. The numerical test indicates that, similar to the Roe scheme, the Van Leer FVS scheme, the Van Leer–Hänel scheme, and AUSM-type schemes do not satisfy the entropy condition and allow expansion shocks at sonic point, when first-order accurate discretizations are used. The Roe scheme, AUSM, AUSM$^+$, and Van Leer–Hänel scheme are not stable due to the presence of the expansion shocks. The Van Leer scheme is stable but yields a strong expansion shock. The FVS scheme of Steger–Warming and the modified Zha–Bilgen scheme yield a small jump at the sonic point. The Edwards LDFSS(2) scheme gives the smoothest results at the sonic point with a very small glitch, when the coarse grid is used. A refined mesh decreases the nonsmoothness of the Steger–Warming scheme, the modified Zha–Bilgen scheme, and the Edwards LDFSS(2) scheme. When second-order MUSCL interpolations are used, all of the schemes obtain accurate results without any expansion shock and nonsmoothness at sonic point. This may imply that using higher than first-order spatial accuracy may generally avoid expansion shocks.

References

[1]Roe, P., "Approximate Riemann Solvers, Parameter Vectors, and Difference Schemes," *Journal of Computational Physics*, Vol. 43, No. 2, 1981, pp. 357–372.

[2]Van Leer, B., "Flux-Vector Splitting for the Euler Equations," *Lecture Note in Physics*, Vol. 170, 1982, pp. 507–512.

[3]Hänel, D., Schwane, R., and Seider, G., "On the Accuracy of Upwind Schemes for the Solution of the Navier–Stokes Equations," AIAA Paper 87-1105, June 1987.

[4]Liou, M.-S., and Steffen, C. J., "A New Flux Splitting Scheme," *Journal of Computational Physics*, Vol. 107, No. 1, 1993, pp. 1–23.

[5]Zha, G.-C., and Bilgen, E., "Numerical Solutions of Euler Equations by Using a New Flux Vector Splitting Scheme," *International Journal for Numerical Methods in Fluids*, Vol. 17, 1993, pp. 115–144.

[6]Zha, G.-C., "Comparative Study of Upwind Scheme Performance for Entropy Conditions and Discontinuities," AIAA Paper 99-3348, June 1999.

[7]Jameson, A., "Analysis and Design of Numerical Schemes for Gas Dynamics I: Artificial Diffusion, Upwind Biasing, Limiters and Their Effect on Accuracy and Multigrid Convergence in Transonic and Hypersonic Flow," AIAA Paper 93-3359, July 1993.

[8]Jameson, A., "Analysis and Design of Numerical Schemes for Gas Dynamics I: Artificial Diffusion, Upwind Biasing, Limiters and Their Effect on Accuracy and Multigrid Convergence in Transonic and Hypersonic Flow," *Journal of Computational Fluid Dynamics*, Vol. 4, No. 3–4, 1995, pp. 171–218.

[9]Jameson, A., "Analysis and Design of Numerical Schemes for Gas Dynamics II: Artificial Diffusion and Discrete Shock Structure," *Journal of Computational Fluid Dynamics*, Vol. 5, No. 1–2, 1995, pp. 1–38.

[10]Liou, M.-S., "Progress Towards an Improved CFD Method: AUSM$^+$," *Proceedings of the AIAA 12th Computational Fluid Dynamics Meeting*, AIAA, Washington, DC, 1995.

[11]Liou, M.-S., "A Sequel to AUSM: AUSM$^+$," *Journal of Computational Physics*, Vol. 129, No. 2, 1996, pp. 364–382.

[12]Edwards, J. R., "A Low-Diffusion Flux-Splitting Scheme for Navier–Stokes Calculations," *Proceedings of the AIAA 12th Computational Fluid Dynamics Meeting*, AIAA, Washington, DC, 1995.

[13]Edwards, J. R., "A Low-Diffusion Flux-Splitting Scheme for Navier–Stokes Calculations," *Computer and Fluids*, Vol. 6, 1997, pp. 635–659.

[14]Osher, S., "Numerical Solution of Singular Perturbation Problems and Hyperbolic Systems of Conservation Laws," *Mathematics Studies*, Vol. 47, 1981, pp. 179–205.

[15]Steger, J. L., and Warming, R. F., "Flux Vector Splitting of the Inviscid Gasdynamic Equations with Application to Finite-Difference Methods," *Journal of Computational Physics*, Vol. 40, No. 2, 1981, pp. 263–293.

[16]Harten, A., Lax, P. D., and Van Leer, B., "On Upstream Differencing and Godunov-Type Scheme for Hyperbolic Conservation Laws," *SIAM Review*, Vol. 25, No. 1, 1983, pp. 35–61.

[17]Roe, P., "Characteristic-Based Schemes for the Euler Equations," *Annual Review of Fluid Mechanics*, Vol. 18, 1986, pp. 337–365.

[18]Van Leer, B., "On the Relation Between the Upwind-Differencing Schemes of Godunov, Enguuist–Osher, and Roe," *SIAM Journal on Scientific and Statistical Computing*, Vol. 5, No. 1, 1984, pp. 1–20.

[19]Mason, M. L., and Putnam, L. E., "The Effect of Throat Contouring on Two-Dimensional Converging–Diverging Nozzles at Static Conditions," NASA TP 1074, 1980.

P. Givi
Associate Editor

Application of a Wavelet Cross-Correlation Technique to the Analysis of Mixing

Maria Vittoria Salvetti* and Giovanni Lombardi*
University of Pisa, 56126 Pisa, Italy
and
François Beux†
Scuola Normale Superiore, 56126 Pisa, Italy

Introduction

THE analysis and control of mixing between two initially segregated streams is of great interest for aerospace, industrial, and environmental applications. A significant example is the mixing between two scalars seeded in two coaxial jets. Although the configuration is apparently simple from the geometrical point of view, the simultaneous presence of two shear layers leads to complex vorticity dynamics, characterized by nonlinear interactions between the structures forming from the instabilities of the two jets. As mixing is strictly connected with the vorticity dynamics, the mechanisms leading to mixing are complex.

The wavelet cross-correlation analysis[1] of the time signals of scalar concentrations can be an effective tool to study the mixing processes in this context. Indeed, this analysis permits the identification of the frequencies and of the time intervals at which the correlation between the fluctuations of the concentrations of the two scalars is high and, hence, mixing is significant. This technique is applied here to the time signals of scalar concentrations deriving from axisymmetric direct numerical simulation of a coaxial jet flow. Because we know that three-dimensional mechanisms play an important role even in the near field of coaxial jets, axisymmetric simulations cannot provide a detailed realistic description of a coaxial jet flow. However, they are well suited to characterize the capabilities of different processing techniques, which can be eventually applied also to three-dimensional simulations to analyze the mixing mechanisms. Moreover, numerical simulation provides simultaneously the time evolution of scalar concentrations and of the vorticity field, so that the mixing processes can be connected to the different events in the vorticity dynamics, such as roll up, passage, and pairing of vortices. Finally, as shown in Ref. 1, the wavelet cross-correlation analysis, if applied to the velocity signals, gives a clear description of the average and instantaneous contributions to the Reynolds stresses from the different events in the vorticity dynamics, which permits us to investigate if the events responsible for mixing are the same giving significant contribution to the Reynolds stress. In particular, although in the simplified context of axisymmetric flows, indications are given on the contribution of the roll up, passage, and pairing of vortical structures to Reynolds stress and to mixing between the two streams.

Received 6 March 1998; revision received 15 October 1998; accepted for publication 18 March 1999.

*Assistant Professor, Dipartimento di Ingegneria Aerospaziale, V. Diotisalvi 2.

†Researcher, Piazza dei Cavalieri 7.

Numerical Setup

As concerns the numerical simulation, the axisymmetric Navier–Stokes equations in cylindrical coordinates (r, z) and in primitive variables have been considered,[2] together with the transport equations for two passive scalars. The numerical method is based on a finite difference scheme, second-order accurate in space and time; details can be found in Refs. 2 and 3.

In the present simulations the ratio between the maximum velocity of the internal and the external jet is $U_c/U_e = 0.67$, and the ratio between the internal and external radius is $R/R_e = 0.517$. The inlet concentration of the first scalar is 1 in the internal jet and 0 elsewhere, and the other has a concentration at the inlet equal to unity in the external jet and equal to 0 elsewhere. The Reynolds number, based on R and U_c, is equal to 1000. At the outflow, radiative boundary conditions are applied to each variable,[2] which permit the simulation of spatially evolving flows. As concerns the external radial boundary, free-slip conditions are assumed. The axial and radial dimensions of the computational domain are, respectively, $16R$ and $10R$. The dimensions of the domain in the present simulations are large enough to avoid spurious effects of the boundary conditions on the dynamics of the jet (see also Ref. 2). The computational grid has 385 points uniformly spaced in the z direction and 305 in the radial direction, with points clustered in high-shear regions.[2] This provides an adequate resolution, by checking the grid independency of the results; the same evolution of the vorticity and scalar fields has been obtained in additional simulations carried out on grids with 769×305 and 385×611 points, respectively. The results are not presented here for the sake of brevity.

Wavelet Cross-Spectral Analysis

Let $W_f(s, \tau)$ and $W_g(s, \tau)$ be, respectively, the continuous wavelet transforms of two time signals $f(t)$ and $g(t)$; s is the inverse of the scale, i.e., the scale number,[1] which plays the same role as the frequency in Fourier analysis, and τ is the translation parameter, corresponding to the position of the wavelet in the physical space. We define the wavelet cross scalogram as $W_{fg}(s, \tau) = W_f^*(s, \tau) W_g(s, \tau)$, where the superscript $*$ denotes the complex conjugate. If the analysis is carried out by means of a complex wavelet, as the Morlet wavelet used herein,[1] the cross scalogram is also complex and can be written in terms of its real and imaginary parts, the coscalogram $\mathrm{Co}W_{fg}$ and the quad-scalogram $\mathrm{Quad}W_{fg}$, respectively. One can see that[1]

$$\int_{-\infty}^{\infty} f(t) g(t)\,\mathrm{d}t = \frac{1}{C_\psi} \int_0^\infty \int_{-\infty}^{\infty} \mathrm{Co}W_{fg}(s, \tau)\,\mathrm{d}\tau\,\mathrm{d}s \tag{1}$$

where C_ψ is the wavelet admissibility constant. If the analysis is applied to the time signals of the concentrations of the two passive scalars, the time intervals and scales at which the fluctuations of the concentrations are correlated can be obtained. Because it is reasonable to assume that high absolute values of the correlation correspond to mixing, the time intervals and scales at which mixing occurs can be identified and connected to the vorticity dynamics.

Results and Discussion

Two typical vorticity fields are shown in Fig. 1. The roll up of the external jet occurs at an almost fixed location, around $z/R = 4$. Although some instabilities of the internal shear layers appear, the roll up of the external shear layer seems to dominate the dynamics of the internal one, at least in the initial zone close to the jet outlet.

The analyzed signals were recorded during the same simulation at different locations and consisted of 16,384 samples, with a sampling time coinciding with the time step of the calculation ($\Delta t = 0.01\ R/U_c$). The initial transient of the flow development after the impulsive start up has been excluded. The results of the wavelet cross-correlation analysis are presented at few locations that are significant with regard to the dynamics of vorticity and mixing.

The first considered location is at $z/R = 6$ and $r/R = 0.96$ and corresponds to significant values of both the correlation between

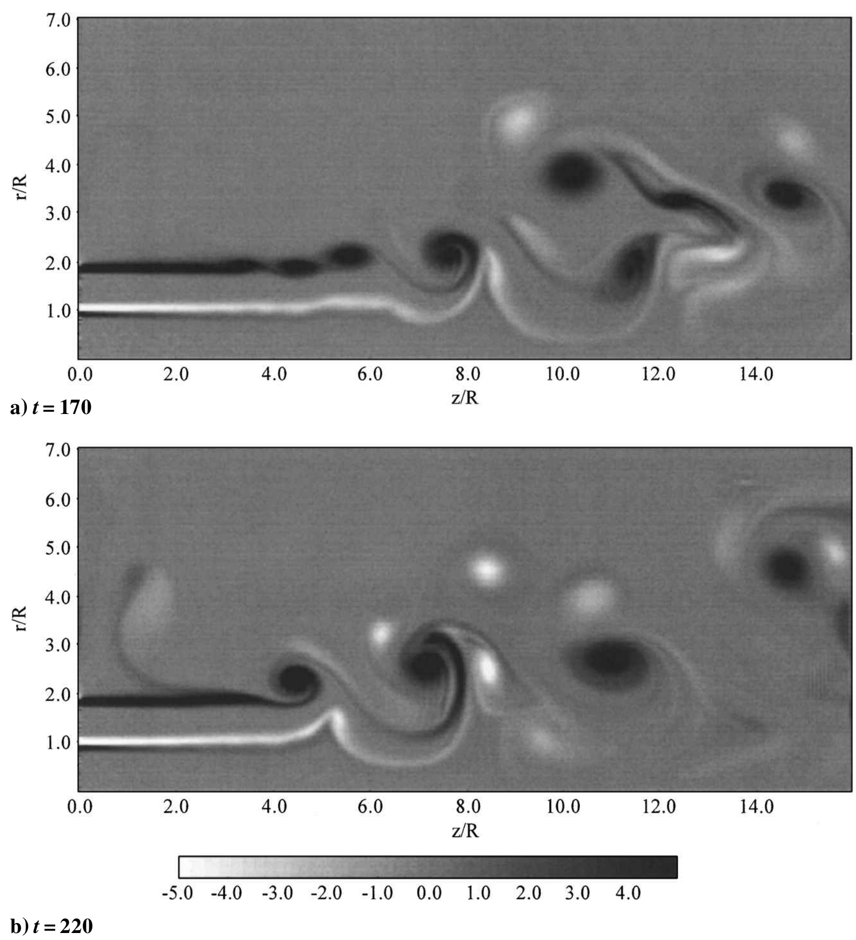

Fig. 1 Vorticity isocontours.

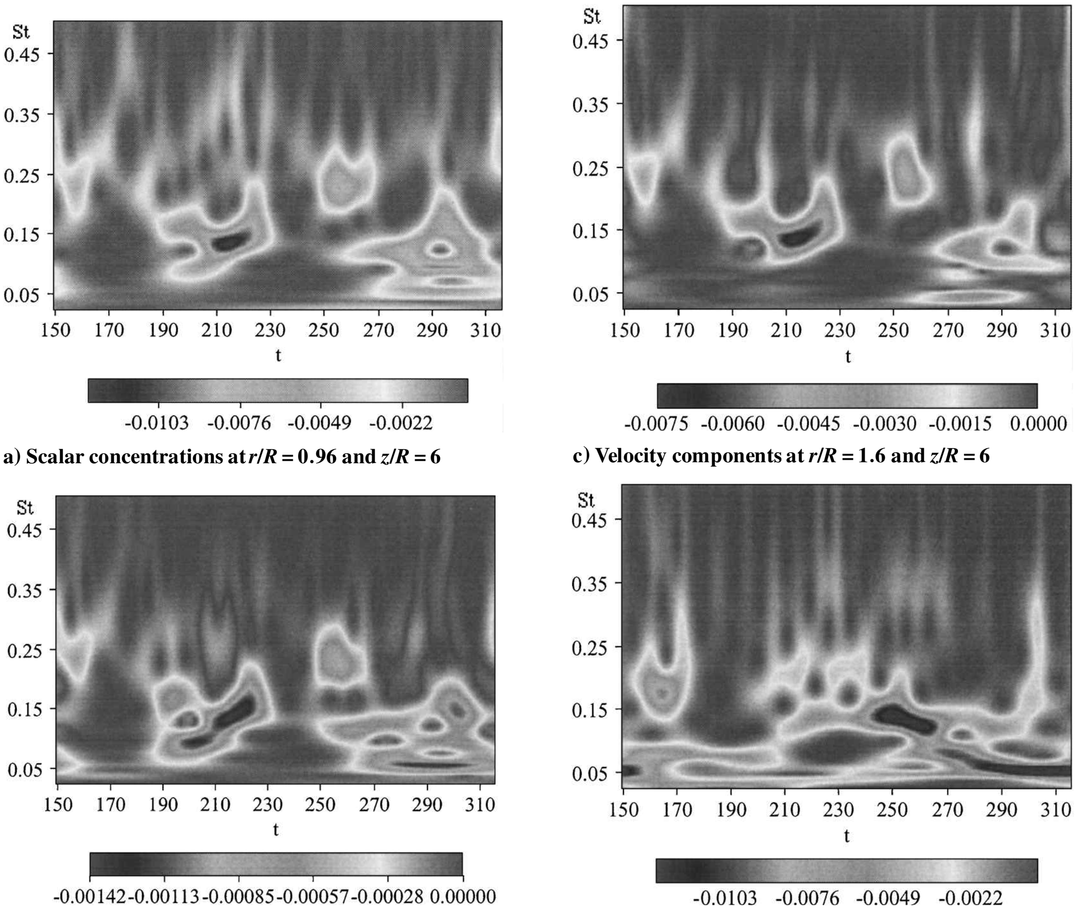

a) Scalar concentrations at $r/R = 0.96$ and $z/R = 6$

b) Velocity components at $r/R = 0.96$ and $z/R = 6$

c) Velocity components at $r/R = 1.6$ and $z/R = 6$

d) Scalar concentrations at $r/R = 0.3$ and $z/R = 10$

Fig. 2 Wavelet coscalograms.

scalar fluctuations $\overline{\xi_1'\xi_2'}$ and Reynolds stress $\overline{uv}$. The wavelet coscalogram of the scalar concentration is shown in Fig. 2a. As already discussed, high values of the wavelet coscalogram coefficients indicate frequencies and time instants that contribute to the correlation between the two signals. In all of the scalograms, the Strouhal number $St = fR/U_c$ is used. The coscalogram of scalar concentration signals, when it does not vanish, is always negative. Conversely, the correlation between u and v can be either positive or negative, depending on the inclination and sign of the vorticity layer; to make the comparison easier, $-|\mathrm{Co}W_{uv}|$ is reported in Fig. 2b. The two scalograms are very similar; this means that, at the considered location, the same events contribute both to the Reynolds stress and to the mixing process. In both scalograms, significant values are observed for Strouhal numbers ranging from $St \simeq 0.05$ to 0.25. The contribution of each frequency is not constant in time. This behavior can be connected with the dynamics of vorticity. At the considered location the vortical structures formed from the roll up of the external layer cause the stretching and the tilting of the internal vorticity layer, yielding thus a significant contribution to the Reynolds stress, as shown also in Ref. 1, and to mixing. The variation of the dominating frequencies is because of the dimensions of these structures. Indeed, higher frequencies correspond to time instants in which the rolled-up vortical structures are small (see, for instance, Fig. 1a). Conversely, lower frequencies (around $St = 0.11$) are found when, at the considered location, the stretching and the tilting of the shear layer is caused by a large vortical structure already formed from the roll up of the external shear layer, as shown for instance from the vorticity fields at $t = 220$ in Fig. 1b.

Let us consider now the position $z/R = 6$ and $r/R = 1.6$, which corresponds to a very high value of $\overline{uv}$ and to negligible correlation between the scalar fluctuations. The coscalogram of the velocity components, shown in Fig. 2c, is qualitatively very similar to that in Fig. 2b, but the values are globally higher. Indeed, at the considered radial location the vorticity layer is elongated and tilted by the same events at $r/R = 0.96$, but, because it is in the external layer, the intensity of the vorticity is higher, and this results in a larger contribution to the Reynolds stress. Conversely, because the mixing between the two scalars occurs mostly because of the stretching of the internal layer between the two jets, no significant contribution to the coscalogram of the scalar concentrations (not shown here for the sake of brevity) is found at this radial location.

Finally, we analyze the signals at $z/R = 10$ and $r/R = 0.3$, where the correlation between the scalar fluctuations is high and $\overline{uv}$ is negligible. The coscalogram of the scalar concentrations is shown in Fig. 2d. As for Fig. 2a, significant values are observed in almost the whole time interval, and the dominant frequencies vary with time. Nevertheless, most of the contribution to the coscalogram in Fig. 2d arises from lower frequencies than in Fig. 2a. Indeed, at the present axial location the mixing is mainly caused by the passage of very large vortical structures just above, which stretch and move the internal layer close to the axis, as can be seen, for instance, from Fig. 1a. This situation does not significantly contribute to $\overline{uv}$ because the intensity of the vorticity is low and, furthermore, the inclination of the layer is negligible.

References

[1]Onorato, M., Jr., Salvetti, M. V., Buresti, G., and Petagna, P., "Wavelet Cross-Correlation Analysis of DNS Velocity Signals in a Coaxial Jet," *European Journal of Mechanics/B Fluids*, Vol. 16, No. 4, 1997, pp. 575–597.

[2]Salvetti, M. V., Orlandi, P., and Verzicco, R., "Numerical Simulations of Transitional Axisymmetric Coaxial Jets," *AIAA Journal*, Vol. 34, No. 4, 1996, pp. 736–743.

[3]Verzicco, R., and Orlandi, P., "A Finite-Difference Scheme for the Three-Dimensional Incompressible Flows in Cylindrical Coordinates," *Journal of Computational Physics*, Vol. 123, No. 2, 1996, pp. 402–414.

P. Givi
Associate Editor